Commun. Comput. Phys.
doi: 10.4208/cicp.OA-2016-0150

Vol. **22**, No. 2, pp. 422-440
August 2017

A Flux-Corrected Phase-Field Method for Surface Diffusion

Yujie Zhang[1] and Wenjing Ye[1,2,*]

[1] *Department of Mechanical and Aerospace Engineering, Hong Kong University of Science and Technology, Hong Kong.*
[2] *Division of Biomedical Engineering, Hong Kong University of Science and Technology, Hong Kong.*

Communicated by Kun Xu

Received 8 September 2016; Accepted (in revised version) 16 December 2016

Abstract. Phase-field methods with a degenerate mobility have been widely used to simulate surface diffusion motion. However, apart from the motion induced by surface diffusion, adverse effects such as shrinkage, coarsening and false merging have been observed in the results obtained from the current phase-field methods, which largely affect the accuracy and numerical stability of these methods. In this paper, a flux-corrected phase-field method is proposed to improve the performance of phase-field methods for simulating surface diffusion. The three effects were numerically studied for the proposed method and compared with those observed in the two existing methods, the original phase-field method and the profile-corrected phase-field method. Results show that compared to the original phase-field method, the shrinkage effect in the profile-corrected phase-field method has been significantly reduced. However, coarsening and false merging effects still present and can be significant in some cases. The flux-corrected phase field performs the best in terms of eliminating the shrinkage and coarsening effects. The false merging effect still exists when the diffuse regions of different interfaces overlap with each other. But it has been much reduced as compared to that in the other two methods.

AMS subject classifications: 82C24

Key words: Phase-field method, surface diffusion, bulk diffusion, profile correction, flux correction.

1 Introduction

Phase-field method is a very useful tool for simulating interfacial phenomena and has been widely used in the modeling of binary alloys [1–3], solidification [4–6], microstruc-

*Corresponding author. *Email addresses:* mewye@ust.hk (W. Ye), yzhangbx@connect.ust.hk (Y. Zhang)

 ©2017 Global-Science Press

https://doi.org/10.4208/cicp.OA-2016-0150 Published online by Cambridge University Press

ture evolutions [7,8] and two-phase flows [9–11]. The major advantages of the phase-field method are its conservation nature and its ability of capturing topological changes naturally. A relatively recent application of the phase-field method is in the simulation of surface diffusion [12–18]. Although it has been proven in [19] that the sharp-interface limit of the Cahn-Hilliard equation with degenerate mobility $M(\phi)=1-\phi^2$ describes the interface motion induced by pure surface diffusion only if the potential is chosen to be logarithmic or double-obstacle form, in practice, a smooth polynomial double-well potential is often used [12–18] in order to avoid singularity. Unfortunately, as remarked by Cahn and Taylor [20], using a biquadratic potential might not drive the phase-field variable ϕ close enough towards ±1 to sufficiently suppress bulk diffusion, a phenomenon which is caused by the normal gradient of the chemical potential and governed by a equation similar to that of quasi-stationary porous medium diffusion [21–23]. As a consequence, some adverse effects have been observed.

Yue et al. [24] pointed out that if a double-well potential was used, the phase-field variable inside/outside of a circular drop would be deviated away from its original value, ±1, and in the meantime the radius of the circular drop would reduce in order to minimize the total energy. This shrinkage effect leads to a volume loss even though mass conservation is satisfied. Another effect caused by using double-well potentials in the phase-field method is the coarsening effect [21–23]. In the presence of the coarsening effect, larger solid domains will grow at the expense of nearby smaller ones. Such a phenomenon should not occur in a motion purely induced by surface diffusion. Different from the shrinkage effect, coarsening effect exists even in the sharp interface limit. In the sharp-interface limit, the interface velocity consists of two terms as shown in (1.1) [21–23]. One comes from the tangential flux, which contributes to the evolution of the interface driven by surface diffusion. The other one comes from a normal flux, which helps to maintain a diffuse interface with a finite thickness, but at the same time, brings the shrinkage and coarsening effects.

$$v_n=\frac{2}{3}\Delta_s\kappa+\frac{1}{4}\mu\nabla_n\mu. \tag{1.1}$$

In order to minimize the shrinkage effect, a profile-corrected phase-field method was proposed in [25] by adding a penalty flux. The function of this additional flux is to enforce a hyperbolic tangent profile of the phase-field variable in order to reduce the volume loss. The overall effect, however, depends on the competition between the original normal flux and the additional penalty flux in shaping the interface profile. In the initial stage of the simulation, the penalty flux is very small and the evolution is dominated by the original normal flux, which deviates the profile from its initial hyperbolic tangent form, resulting in a volume loss in most cases. Only when the deviation is sufficiently large, the effect of the penalty flux becomes stronger and it competes with the original normal flux to restore the profile back to the hyperbolic tangent form. The final profile, and thus the volume loss, is determined by the net effect of the two fluxes. In addition, as in the original phase-field method, the cause of the coarsening effect, that is, the bulk diffusion motion brought by the normal flux, still presents in the profile-corrected phase-

https://doi.org/10.4208/cicp.OA-2016-0150 Published online by Cambridge University Press

field method. Hence the coarsening effect still exists. These two observations motivate us to propose a new method entitled flux-corrected phase-field method. In this method, instead of adding the penalty flux, we replace the original normal flux by the penalty flux so to remove the source of the coarsening effect. Apart from the two adverse effects, we have also observed that the performance of both the original phase-field method and the profile-corrected phase-field method deteriorates in cases with adjacent interfaces, similar to what has been observed in the level set method [26–30]. When two interfaces are close by, the diffuse regions of the interfaces overlap with each other, which lead to false merging of the interfaces. In this paper, this phenomenon will be discussed and the performances of the three methods: the original phase-field method, the profile-corrected phase-field method and the flux-corrected phase-field method, in the simulation of problems with adjacent interfaces will be presented and compared.

This paper is organized as follows. In Section 2, we describe the original phase-field method, the profile-corrected phase-field method and our proposed flux-corrected phase field. It is followed by a brief description of the numerical scheme. In Section 3, we first present the studies of the shrinkage, coarsening and false merging effects in the three methods, then compare the accuracies of the three methods through three benchmark examples for surface diffusion. The study of the parameter A in both profile-corrected and flux-corrected phase-field methods is also presented in this section. The paper is concluded with a summary section.

2 Methodologies

In this section, the original phase-field method is introduced first, followed by the profile-corrected phase-field method [25] and the flux-corrected phase-field method. The numerical scheme is presented last.

2.1 Original phase-field method

The Cahn-Hilliard equation with degenerate mobility is the most commonly used phase-field model to describe interface evolution caused by surface diffusion [12–16, 31]. The phase-field variable ϕ is governed by

$$\frac{\partial \phi}{\partial t} = -\nabla \cdot \overrightarrow{J}, \tag{2.1}$$

$$\overrightarrow{J} = -M(\phi)\nabla \mu, \tag{2.2}$$

$$\mu = -\varepsilon^2 \Delta \phi + f'(\phi), \tag{2.3}$$

$$f(\phi) = \frac{1}{4}(1-\phi^2)^2, \tag{2.4}$$

$$M(\phi) = |1-\phi^2|, \tag{2.5}$$

https://doi.org/10.4208/cicp.OA-2016-0150 Published online by Cambridge University Press

where $\overrightarrow{J}$ is the flux; $M(\phi)$ is the degenerate mobility; μ is the chemical potential; ε is the interfacial tension which determines the width of the interface; and ϕ is the bulk free energy. In this model, the interface is located at the contour of $\phi=0$, and ϕ retains to ±1 in the two pure phases. Due to the use of the double-well potential, (2.4), two artificial effects have been observed in the results obtained from this model: the shrinkage effect [24,25] and the coarsening effect [21–23]. The shrinkage effect is caused by the deviation of ϕ from ±1 in the bulk phases, and this effect will eventually lead to volume loss even though mass is conserved. Coarsening effect arising from bulk diffusion couples disjoint solid domains with each other such that larger solid domains grow at the expense of smaller ones [22].

2.2 Profile-corrected phase-field method

To conserve the volume enclosed by the interface as required in surface diffusion, a profile-corrected phase-field method was proposed [25]. The basic idea of the method is to maintain the hyperbolic tangent property of the interface profile. This was done by adding a penalty flux into the original flux as shown in

$$\frac{\partial\phi}{\partial t}=-\nabla\cdot\overrightarrow{J}-\nabla\cdot\overrightarrow{J_P}, \tag{2.6}$$

$$\overrightarrow{J_P}=-\lambda M(\phi)\Big(\nabla\phi-\frac{1}{A\varepsilon}(1-\phi^2)\frac{\nabla\phi}{|\nabla\phi|}\Big), \tag{2.7}$$

where $\overrightarrow{J}$ is the original flux in the phase-field method shown in (2.2); $\overrightarrow{J_P}$ is the penalty flux used to maintain the ϕ profile at the interface to be $tanh(\frac{d}{A\varepsilon})$; λ is a parameter controlling the magnitude of the penalty flux; A is a parameter that controls the slope of the profile; d is the corresponding signed distance function of the interface. A common choice of A is $\sqrt{2}$ due to the fact that $\tanh(\frac{d}{\sqrt{2}\varepsilon})$ is the steady interface profile for flat surfaces [25]. Here, we should notice that the added penalty flux will not alternate the sharp-interface limit, as the leading order solution of original phase-field equation is hyperbolic tangent form, which will give zero penalty flux. Also, in the sharp-interface limit, the volume loss of the original phase-field method tends to zero and the profile-corrected phase-field method will be expected to obtain the same results with the original phase-field method.

2.3 Flux-corrected phase-field method

The structure of the interface plays an important role in volume conservation [24,25] and thus affects the accuracy of the phase filed method in simulating surface diffusion. The interfacial profile in the original phase filed method is controlled by the mixing energy:

$$E(\phi)=\int_\Omega\Big(f(\phi)+\frac{\varepsilon^2}{2}|\nabla\phi|^2\Big)d\boldsymbol{x}. \tag{2.8}$$

https://doi.org/10.4208/cicp.OA-2016-0150 Published online by Cambridge University Press

The competition between the phobic effect arising from the bulk energy $f(\phi)$, which produces the classical sharp-interface, and the philic effect from the gradient term which diffuses ϕ away from the interface into bulk regions, determines the finite thickness of the diffuse interface profile [32]. The profile generated by this mixing energy unfortunately cannot preserve the hyperbolic tangent form, which leads to volume loss [25]. In the profile-corrected phase-field method, a penalty normal flux is added in order to restore such a form. In this method, two sources exist in shaping the interface profile: the original flux $\overrightarrow{J}$ and the penalty flux $\overrightarrow{J_P}$. It is the original normal flux which contributes mostly in diffusing the interface in the normal direction and competes with the penalty flux. This competition affects the accuracy and the stability of the numerical scheme. In addition, as discussed in [21–23], the original normal flux also brings in nonlinear bulk diffusion, an unwanted effect in simulating surface diffusion. Hence in the proposed flux-corrected phase-field method, the original normal flux is removed and replaced with the penalty flux. The equations are listed as follows:

$$\frac{\partial\phi}{\partial t}=-\nabla\cdot\overrightarrow{J_M}, \tag{2.9}$$

$$\overrightarrow{J_M}=\overrightarrow{J}-\overrightarrow{J_n}+\overrightarrow{J_P}, \tag{2.10}$$

$$\overrightarrow{J_P}=-\lambda M(\phi)\Big(\nabla\phi-\frac{1}{A\varepsilon}(1-\phi^2)\frac{\nabla\phi}{|\nabla\phi|}\Big), \tag{2.11}$$

where $\overrightarrow{J_n}=(\overrightarrow{J}\cdot\overrightarrow{n})\,\overrightarrow{n}$ is the normal component of the flux.

2.4 Numerical scheme

In this work, we adopt an efficient and accurate semi-implicit numerical scheme to discretize phase-field equations [14]:

$$\frac{\phi^{n+1}-\phi^n}{\Delta t}=B\varepsilon^2\Delta^2(\phi^n-\phi^{n+1})+S\Delta(\phi^{n+1}-\phi^n)-\nabla\cdot\overrightarrow{J_R^n}, \tag{2.12}$$

where B and S are two positive stabilizing parameters. B is chosen to be 1.0. S is 0.5 in the original phase-field method and the profile-corrected phase-field method, and $S=0.0$ for the flux-corrected phase-field method. The different choice of S for the flux-corrected phase-field method is due to the following reason. We realize that the stabilization term $S\Delta(\phi^{n+1}-\phi^n)$ is mainly used to filter out the oscillations caused by the normal flux. In our approach, the normal flux is removed and hence there is no need to keep this term. Indeed, our numerical investigation shows that $S=0.0$ gives the best performance. However for the original and profile-corrected phase-field methods, since the normal flux exists, the S term has to be there. If we set $S=0.0$, the numerical scheme will be less stable. For the original phase-field method, $\overrightarrow{J_R^n}=\overrightarrow{J^n}=-M(\phi^n)\nabla(-\varepsilon^2\Delta\phi+\phi^3-\phi)$. For the profile-corrected phase-field method, $\overrightarrow{J_R^n}=\overrightarrow{J^n}-\lambda M(\phi^n)(\nabla\phi^n-\frac{1}{A\varepsilon}(1-(\phi^n)^2)\frac{\nabla\phi^n}{|\nabla\phi^n|})$. For

https://doi.org/10.4208/cicp.OA-2016-0150 Published online by Cambridge University Press

the flux-corrected phase-field method, $\overrightarrow{J_R^n} = \overrightarrow{J^n} - (\overrightarrow{J^n} \cdot \frac{\nabla\phi^n}{|\nabla\phi^n|}) \frac{\nabla\phi^n}{|\nabla\phi^n|} - \lambda M(\phi^n)(\nabla\phi^n - \frac{1}{A\varepsilon}(1-(\phi^n)^2)\frac{\nabla\phi^n}{|\nabla\phi^n|})$.

For the spatial discretization, we applied the standard cosine pseudospectral method and performed real-even symmetry discrete Fourier transform (DFT) in both x and y directions. Interested readers can refer to FFTW [33] for more information about the implementation of DFT.

3 Results and discussions

The performance of the flux-corrected phase-field method was first evaluated by examining the three effects, namely the shrinkage, the coarsening and the false merging effects. The accuracy of the method was then checked and compared with that of the original phase-field and profile-corrected phase-field methods using examples involving the evolution of an ellipse, a lobed-star and a 3D complex shapes under surface diffusion. For benchmark solutions, the front tracking method [34] and the level-set method [35] were employed to obtain the sharp interface limit of the solutions. Under surface diffusion, the evolution of the interface is governed by

$$\frac{d\boldsymbol{X}}{dt} = V_n \boldsymbol{n}, \tag{3.1}$$

where $\boldsymbol{X} = (x(s,t), y(s,t))$ represents a point on the interface, s is a parameter of the interface, t is time, $V_n = \frac{\partial^2 \kappa}{\partial s^2}$ is the normal velocity, κ is the curvature and $\boldsymbol{n}$ is the outward normal vector. In the front tracking method, V_n is calculated by the finite difference method and (3.1) is updated using the explicit Euler scheme. The mesh size is adjusted so that the minimum and the maximum distances between adjacent points are 0.025 and 0.1 respectively. For simplicity, a constant time step of 1.0×10^{-12} is chosen for all cases in the simulations using the front tracking method. This time step is sufficiently small to ensure stability.

3.1 Shrinkage effect

The shrinkage effect of Cahn-Hilliard equation with a double-well potential has been pointed out and studied on a circular drop under surface diffusion [24]. During the evolution, the initial circular drop tends to lower its energy by shrinking its radius, in the meantime, the bulk ϕ shifted slightly away from its initial value to satisfy mass conservation. According to the analysis in [24], the shrinkage of the radius of the circular drop is proportional to the interfacial thickness:

$$\delta r = -\frac{\sqrt{2}V}{24\pi}\frac{\varepsilon}{r_0^2}, \tag{3.2}$$

https://doi.org/10.4208/cicp.OA-2016-0150 Published online by Cambridge University Press

where δr is the change of the radius; V is the total simulation volume; r_0 is the initial radius and ε indicates the interfacial thickness.

To investigate the shrinkage effect in the three method, the same problem was considered in this work. The evolution of a circle with an initial radius of $r_0 = 1.0$ located in the center of the domain $[0,4]\times[0,4]$ was simulated using the three methods. Fig. 1 plots the shrinkage of the radius as a function of ε. The theoretical prediction of the final shrinkage of the circle, (3.2), is also plotted for comparison. The results obtained from the original phase-field method match quite well with the theoretical predictions, exhibiting a shrinkage that is proportional to the interfacial thickness. In the profile-corrected phase-field method, due to the added penalty flux, the shift of ϕ in the bulk region is limited. Hence the shrinkage of the circle is reduced particularly near the sharp interface limit, as demonstrated in Fig. 1. For a circle shape, because of symmetry, only normal flux exists and there is no tangent flux, hence there should be no shrinkage effect in the results obtained from the flux-corrected phase-field method, which indeed is illustrated in the figure. Those small values that are on the order of 10^{-5} are in fact not the shrinkages of the radius. They are the numerical errors in the calculation of the radius, which can be justified in Fig. 2, where the change of the radius as a function of time simulated by the flux-corrected phase-field method with $\varepsilon = 0.1$ is plotted. The constant profile indicates no shrinkage during evolution.

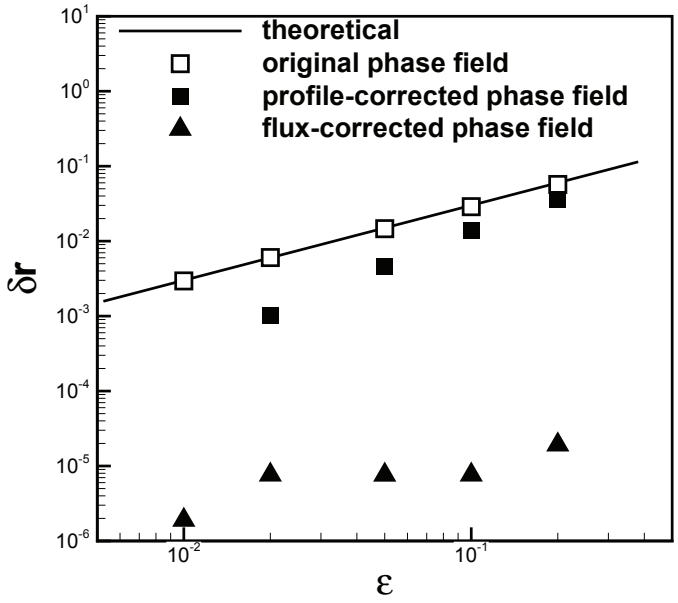


Figure 1: Shrinkage of the radius of a circle as a function of under surface diffusion. $\lambda = 0.2$ for both the profile-corrected and the flux-corrected phase-field methods. Mesh size is 512×512 for $\varepsilon = 0.2, 0.1, 0.05, 0.02$ and 1024×1024 for $\varepsilon = 0.01$. The missing data point at $\varepsilon = 0.01$ of the profile-corrected phase field method is due to the fact that the corresponding result is unstable under such small epsilon.

https://doi.org/10.4208/cicp.OA-2016-0150 Published online by Cambridge University Press

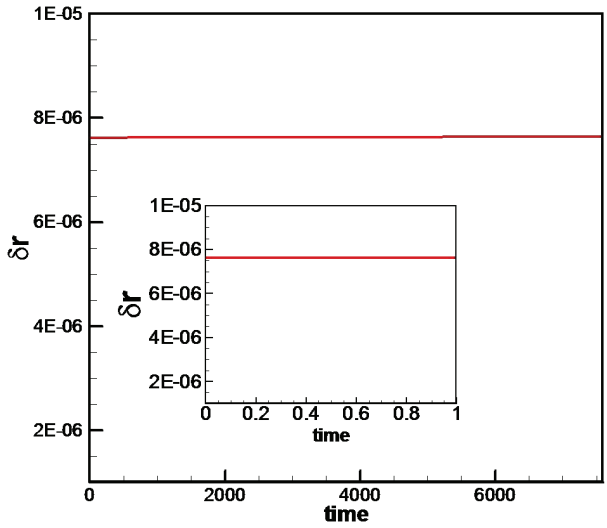


Figure 2: Change of the radius as a function of time under surface diffusion simulated by the flux-corrected phase-field method with $\varepsilon=0.1$.

3.2 Coarsening effect

To investigate the coarsening effect, we consider two circles with different radius r_1 and r_2 located at a distance of d away, as shown in Fig. 3. In the simulation, $r_1=0.3$, $r_2=0.1$, $d=0.5$, $h=1.0$, $\varepsilon=0.01$, $\lambda=1.0$ and $A=\sqrt{2}$. The mesh size was chosen to be 128×256 and

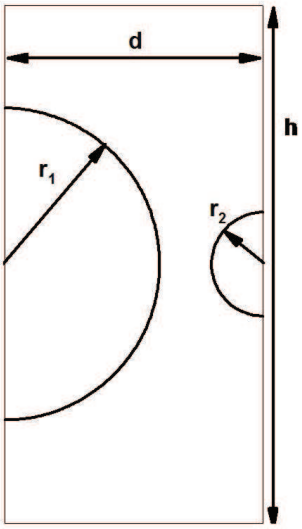


Figure 3: Schematic illustration of the simulation domain of the two circles.

https://doi.org/10.4208/cicp.OA-2016-0150 Published online by Cambridge University Press

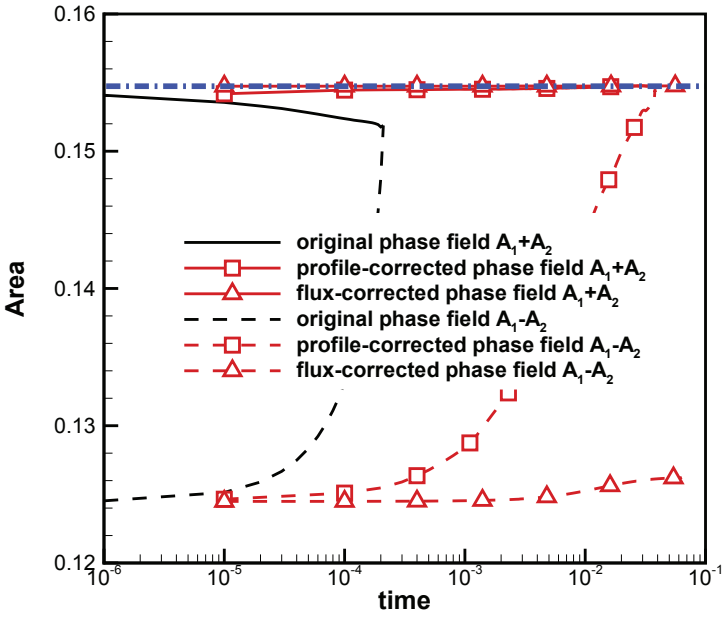


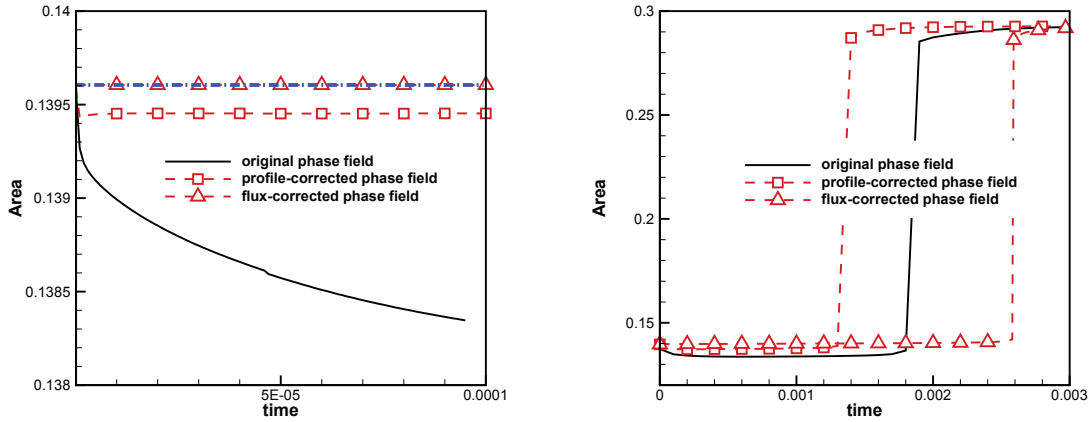
Figure 4: The sum and the difference of areas of two half circles as functions of time. A_1 is the area of the half large circle and A_2 is the area of the half small circle. The blue dash-dot line indicates the initial total area.

the time step was 1.0×10^{-6}. The areas of the two half circles A_1 and A_2 were calculated. The sum and the difference of the two areas, A_1+A_2 and A_1-A_2, are plotted in Fig. 4 as functions of time. A_1+A_2 gives the total area, which reflects the shrinkage effect, and A_1-A_2 reflects the coarsening effect. From the results shown in Fig. 4, it is very clear that there are strong shrinkage and coarsening effects in the results obtained from the original phase-field method, and the smaller circle disappears at $t=2.0\times10^{-4}$, indicated by the interception of "A_1+A_2" & "A_1-A_2" curves. Compared to the original phase-field method, the coarsening effect is much reduced in the profile-corrected phase-field method, which is reflected in the fact that the smaller circle disappears at a much later time 4.0×10^{-2}. However, the coarsen effect still presents and is quite strong. For the flux-corrected phase-field method, results show almost no shrinkage effect and very little coarsening effect, indicating the effectiveness in removing the source of both effects in the flux-corrected phase-field method.

3.3 False merging effect

The problem used to study the false merging effect is the same as that of Section 3.2, but with different parameters. In order to separate the false merging effect from the coarsening effect, two circles with the same radius, $r_1=r_2=0.3$, were considered. Other parameters are $d=0.8$, $h=1.0$, $\lambda=1.0$ and $A=\sqrt{2}$. The mesh size used in the simulation

https://doi.org/10.4208/cicp.OA-2016-0150 Published online by Cambridge University Press



(a) $\varepsilon=0.01$ (b) $\varepsilon=0.01$

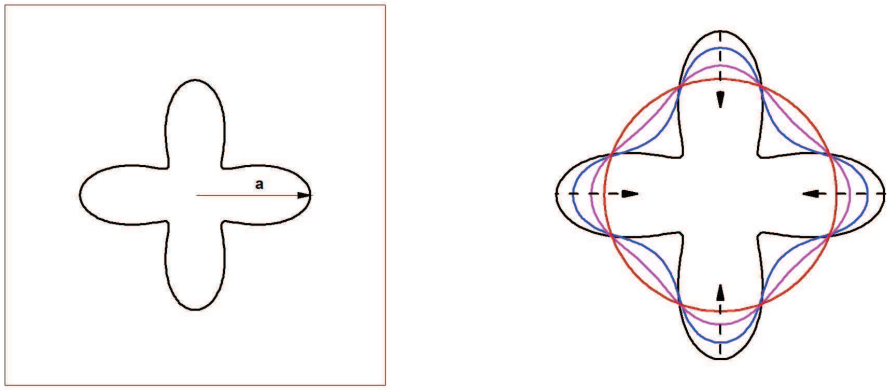
Figure 5: Area of one half circle as a function of time. (a) $\varepsilon=0.01$, the blue dash-dot line indicates the initial area; (b) $\varepsilon=0.05$.

was 205×256 and the time step was 1.0×10^{-6}. Fig. 5 shows the area of one half circle as a function of time for cases with $\varepsilon=0.01$ and $\varepsilon=0.05$. When ε is small, that is, $\varepsilon=0.01$, the two circles are far away from each other, and the evolution of each circle is independent of each other indicated by either the reduced or constant area over time shown in Fig. 5(a). Fig. 5(a) also shows a strong shrinkage effect in the original phase-field method. This effect has been significantly suppressed in the profile-corrected phase-field method. Other than the initial drop, the area of the circle remains almost unchanged over the time. The flux-corrected method shows no any shrinkage effect over the entire simulation time. With a thick interface, for example, $\varepsilon=0.05$, the diffuse regions of the two circles overlap, and the two circles start to influence each other, leading to a merging eventually, which is indicated by a sudden increase in the area as shown in Fig. 5(b). Since both the normal flux and the added penalty flux contribute to the merging, the merging took place much earlier in the profile-corrected phase-field method than that in the original method where only normal flux exists. For the flux-corrected phase-field method, the normal flux was removed. Hence the merging occurs at a much later time, but unfortunately still exists due to the penalty flux.

3.4 Ellipse & 4-lobed-star shapes

In the previous sections, the performances of the three methods were compared with regarding to the three adverse effects. Results have shown that the newly proposed method, the flux-corrected phase-field method, performs the best. In this section, the accuracy of the three methods is further examined and compared. Non-circular shapes such as ellipse and 4-lobed star were chosen as the benchmark problems and results obtained from the front tracking method were used as reference solutions.

https://doi.org/10.4208/cicp.OA-2016-0150 Published online by Cambridge University Press



(a) (b)

Figure 6: (a) Initial shape of the 4-lobed star; (b) Evolution of the 4-lobed star at $t=0$, 1×10^{-5}, 2×10^{-5}, 1×10^{-4}.

The initial shape of the ellipse is defined as follows

$$\frac{(x-0.5)^2}{a^2}+\frac{(y-0.5)^2}{b^2}=1 \tag{3.3}$$

with $a=0.3$ and $b=0.2$.

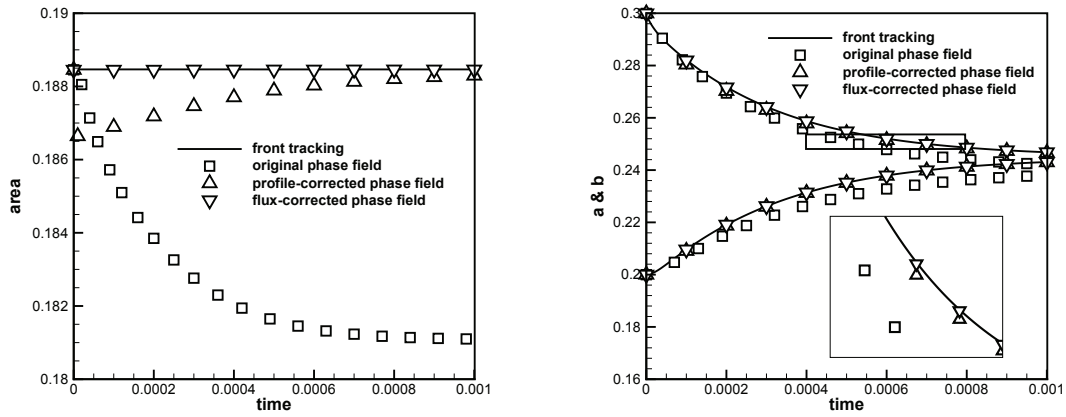
The initial shape of the 4-lobed star illustrated in Fig. 6(a) is given by

$$\begin{aligned} r&=r_0+\Delta r\cdot\cos(n\theta),\\ x(\theta)&=r\cdot\cos\theta,\\ y(\theta)&=r\cdot\sin\theta \end{aligned} \tag{3.4}$$

with $r_0=0.2$, $\Delta r=0.1$, and $n=4$.

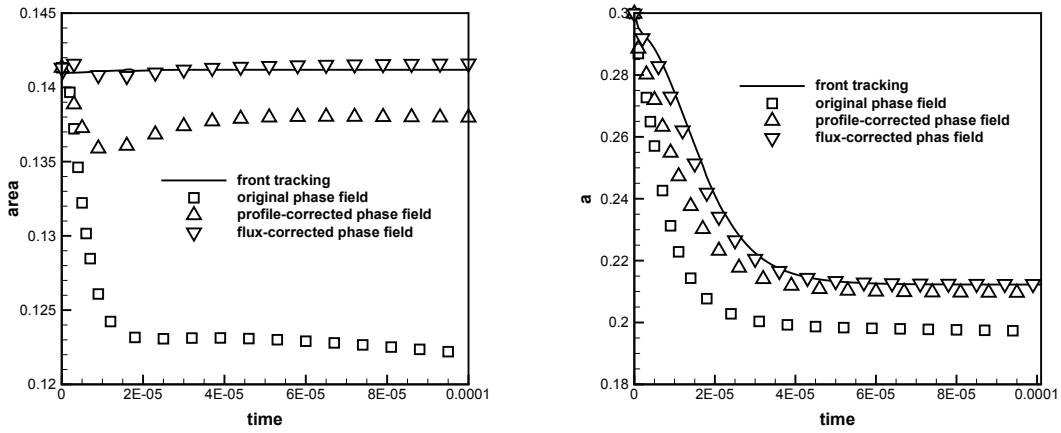
The simulation domain was $[0,1]\times[0,1]$ and the mesh size was 128×128. The interfacial tension was set as $\varepsilon=\frac{m\Delta x}{2A\cdot\tanh^{-1}(0.9)}$, where $m=16$ is the number of grids across the diffuse region of the interface. The time steps used for the ellipse and 4-lobed star are 1×10^{-6} and 1×10^{-7} separately, which are much larger than the time in the explicit method, required by the fourth-order CFL restriction (in the order of 1×10^{-9}). And this is actually achieved by the adopting of the stabilizing terms and semi-implicit scheme in (2.12). The evolutions of both shapes were simulated using three methods. The evolved shapes of the 4-lobed star at different time instances were illustrated in Fig. 6(b). Fig. 7 and Fig. 8 plot the changes of some major parameters such as the area, the major axis and the minor axis of the two shapes over time obtained from various methods. In both examples, the flux-corrected phase-field method conserved the volume the best. For the ellipse shape, both the profile-corrected and the flux-corrected phase-field methods were able to simulate the major and the minor axes accurately with the flux-corrected method

https://doi.org/10.4208/cicp.OA-2016-0150 Published online by Cambridge University Press



(a) (b)

Figure 7: Comparison of some major parameters of the ellipse evolved over time under surface diffusion: (a) change in the area over time; (b) changes in the major and minor axes over time. Time step is 1.0×10^{-6}; $\lambda=2.0$; $A=1.0$.



(a) (b)

Figure 8: Comparison of some major parameters of the 4-lobed star evolved over time under surface diffusion. (a) change of area over time; (b) change of a over time. Time step is 1.0×10^{-7}; $\lambda=1.0$; $A=1.0$.

performed slightly better. However, for more complex shapes such as the 4-lobed star shape, the accuracy of the profile-corrected phase-field method deteriorated particularly at the initial stage. This is caused by the strong bulk diffusion, resulting in a false additional velocity proportional to $\kappa\nabla_n\kappa$ at the interface, due to the large gradient of curvature along the interface. The flux-corrected phase-field method still performed well since the source of the bulk diffusion, the original normal flux, was removed. In both examples, the accuracy of the original phase-field method was unsatisfactory.

https://doi.org/10.4208/cicp.OA-2016-0150 Published online by Cambridge University Press

3.5 Effect of A parameter

An important parameter in both the profile-corrected method and the flux-corrected method is A, which controls the slope of the profile. Due to the competition between the original normal flux and the penalty flux in the profile-corrected phase-field method, the choice of A will affect the accuracy and the stability of the scheme. For flat surfaces, the original normal flux leads to a hyperbolic tangent profile $\tanh(\frac{d}{\sqrt{2}\varepsilon})$. By setting $A=\sqrt{2}$, the competition between the original normal flux and the penalty flux is minimized, and this is the main reason why A was chosen to be $\sqrt{2}$ in pervious work. However, for general curved interfaces, the diffused interfacial profile caused by the original normal flux is no longer $\tanh(\frac{d}{\sqrt{2}\varepsilon})$, and is generally difficult to predict its accurate form. Based on the assumption that the profile should not deviate too much from $\tanh(\frac{d}{\sqrt{2}\varepsilon})$, a common practice is to still set $A=\sqrt{2}$ or in some cases $A=1$. Such a choice seems to work quite well in the examples shown in the previous sections. It is likely not the optimal choice, and a systematic selection method for A for general problems is yet to come. On the other hand, due to the removable of the competition, the performance of the flux-corrected phase-field method should not depend too much on the value of A.

The influence of the choice of A on the accuracy of the profile- corrected phase-field method and flux-corrected phase-field method was investigated on the ellipse example of Section 3.4. The simulation domain was chosen to be $[0,1]\times[0,1]$ and the mesh size was 128×128. $\varepsilon=\frac{m\Delta x}{2A\cdot\tanh^{-1}(0.9)}$ with $m=16$ being the number of grids across the diffuse region of the interface. For the choice of λ, numerical studies indicate that, a constant of λ_0 works well for the profile-corrected phase field, and $\lambda=\lambda_0/A^2$ works well for the flux-corrected phase-field method. λ_0 was chosen to be 2.0 in both cases.

Fig. 9 shows the evolution of the ellipse shape under surface diffusion simulated with different values of A. Results obtained from the profile-corrected method are presented in Fig. 9(a), from which it is very clear that the accuracy depends on the choice of A. With $A=1.0$ the method performed the best. When A is larger than 2.0 or too smaller than 0.5, the error becomes significant, and when A is equal to 4.0, the scheme ever becomes unstable. The accuracy of the flux-corrected method shows a much reduced dependence on the value of A, which is demonstrated in Fig. 9(b), where the time evolution of the major and the minor axes of the ellipse are plotted for different choices of A ranging from 0.5 to 4. All curves match with the reference result very well.

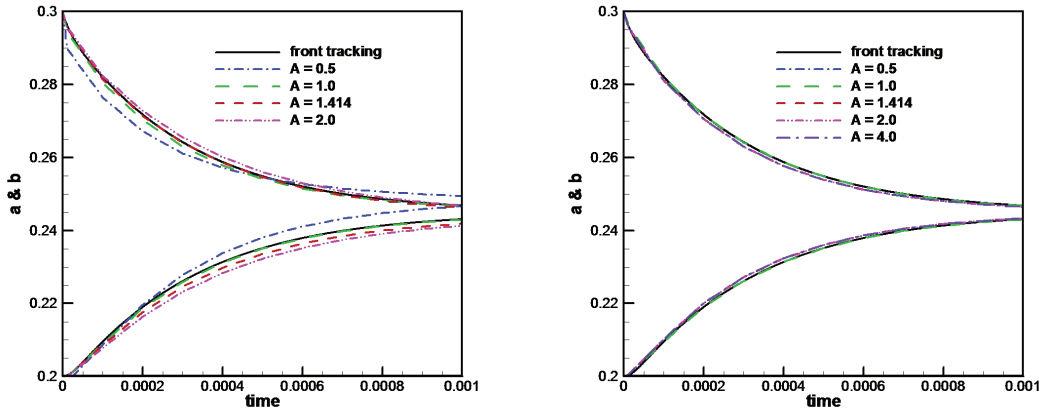
To further demonstrate the competition effect in the profile-corrected phase-field method, we choose a different profile to approximate the diffusive region of the interface:

$$\phi=\frac{2}{\pi}\arctan\left(\frac{d}{A\varepsilon}\right). \tag{3.5}$$

The corresponding penalty flux is

$$\overrightarrow{J_P}=-\lambda M(\phi)\left(\nabla\phi-\frac{1}{A\varepsilon}\frac{2}{\pi}\cos^2\left(\frac{\pi}{2}\phi\right)\frac{\nabla\phi}{|\nabla\phi|}\right). \tag{3.6}$$

https://doi.org/10.4208/cicp.OA-2016-0150 Published online by Cambridge University Press



(a) (b)

Figure 9: Simulated evolution of an ellipse shape under surface diffusion with different choice of A. (a): profile-corrected phase-field method; (b): flux-corrected phase-field method.

In this case, the competition in the profile-corrected phase-field method should be very strong, because the original normal flux tends to approach a hyperbolic tangent-like profile, while the penalty flux leads to a profile of a different type. Fig. 10 shows the comparison of the ellipse evolution under surface diffusion when the penalty flux of (3.6) is adopted. The agreement between the results from the flux-corrected phase-field method and the reference result is almost perfect, while those from the profile-corrected phase-

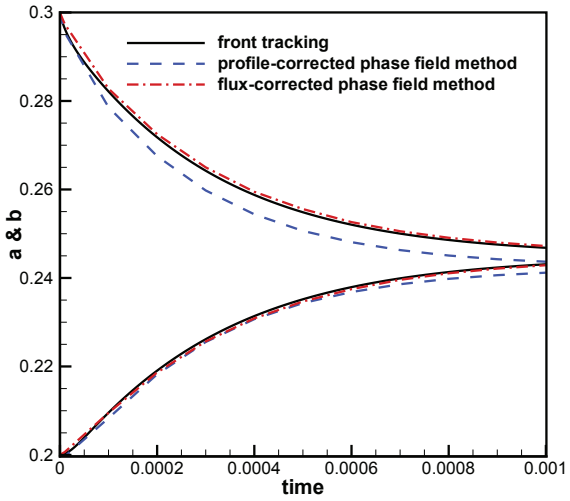


Figure 10: Comparison of ellipse evolution under surface diffusion simulated with the penalty flux of (3.6). $A=1.0$; Mesh size is 128×128; Time step is 1.0×10^{-6}; $\varepsilon=\frac{16\Delta x}{2A\cdot tan(0.9\pi/2)}$.

https://doi.org/10.4208/cicp.OA-2016-0150 Published online by Cambridge University Press

field method deviates significantly from the reference solutions. This further indicates that in the profile-corrected method, the penalty flux needs to be carefully selected in order to reduce the strong competition between itself and the original normal flux, and thus to reduce errors, while in the flux-corrected method, the performance is much less dependent on the choice of the penalty flux, indicating the robustness of the method.

3.6 3D complex shape

In this section, the results of the evolution of a 3D object with complex shape under surface diffusion are presented. The initial shape is defined implicitly by the following equation,

$$\begin{aligned} f=&((x^2+y^2-C^2)^2+(z-1)^2(z+1)^2)((y^2+z^2-C^2)^2\\ &+(x-1)^2(x+1)^2)((x^2+z^2-C^2)^2+(y-1)^2(y+1)^2)-1=0. \end{aligned} \tag{3.7}$$

The simulation domain was $[0,4]\times[0,4]\times[0,4]$ and the mesh size is $64\times64\times64$. The time step is chosen to be $\Delta t=1\times10^{-4}$. The same problem has been investigated in [35] and [36] using the level-set method. For this case, the evolution of the shape involves complex topological changes, which likely induce strong coarsening effects in phase-field methods. Here, it serves a good benchmark problem for testing the performance of phase-field methods. Results obtained by the level-set method [35] are used as reference solutions, which are free of any coarsening effect. It has been shown in [35] and [36], after the complex topological change, the initial complex 3D object eventually evolves into a hollow sphere. The simulated evolution of this complex shape under surface diffusion by the original phase field, the profile-corrected phase field and the flux-corrected phase field are shown in Fig. 11. From Fig. 11, it is clear that the strong coarsening effect, originating form the large curvature gradient along the interface, makes the original phase field evolve much faster than the actual motion induced by surface diffusion [35]. The final shape, that is, a solid sphere predicted by the original phase field is simply incorrect. Although the profile-corrected phase field method slows down the process, giving a better evolution than the original phase field method, the final topology predicted is also a solid sphere, which is incorrect. On the other the flux-corrected phase field method gives the best performance. Not only does it accurately capture the entire evolution process, but also gives the correct topology of the final structure. Fig. 12 plots the cross-sections of the final shape obtained by the three phase-field methods as well as the reference solutions, which further illustrates the good performance of the flux-corrected phase-field method.

4 Summary

In this paper, a flux-corrected phase-field method is proposed to improve the performance of phase-field methods in the simulation of surface diffusion. Studies of three

https://doi.org/10.4208/cicp.OA-2016-0150 Published online by Cambridge University Press

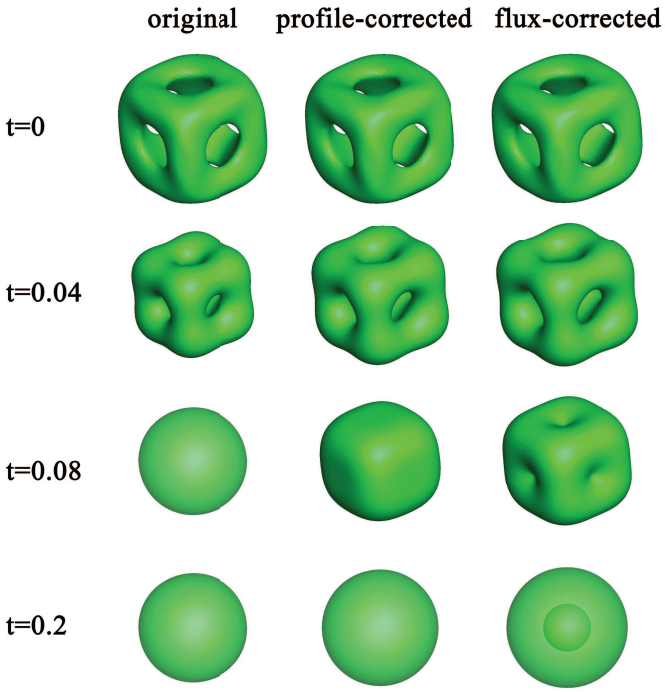


Figure 11: The evolution of a complex 3D shape under surface diffusion. Results obtained from the original, the profile-corrected and the flux-corrected phase field methods are presented in the first, the second and the third columns respectively.

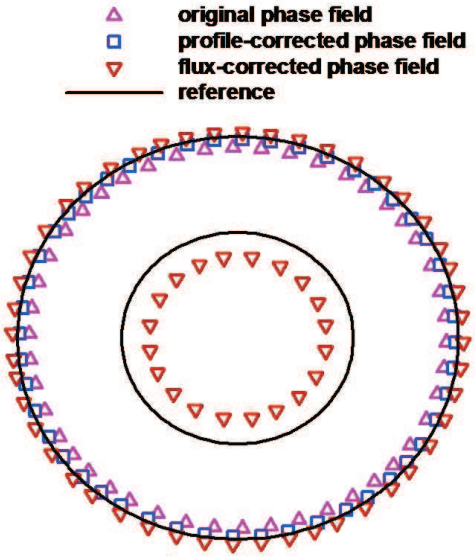


Figure 12: Comparison of the final cross-sections obtained by three phase field methods. The reference solutions are obtained by the level set method [35], which is free from any coarsening effect.

https://doi.org/10.4208/cicp.OA-2016-0150 Published online by Cambridge University Press

effects commonly observed in the phase-field methods, namely the shrinkage, the coarsening and the false merging effects, have been conducted, and results show that even though the introduced penalty flux in the profile-corrected phase-field method is able to reduce volume loss significantly, due to the competition between the original normal flux and the penalty flux, volume loss can still be observed particularly during the initial stage. In addition, coarsening effect still presents and is quite strong due to the original normal flux, which causes nonlinear bulk diffusion. In the flux-corrected phase-field method, by removing the original normal flux and replacing it with the penalty flux, the non-linear bulk diffusion and the competition between the original normal flux and the penalty flux in the profile-corrected phase-field method are eliminated, resulting in a much improved performance in all three aspects. The accuracy of the proposed method is further demonstrated on three benchmark problems: the evolution of an ellipse, a 4-lobed star and a 3D complex shapes. Results have shown that among the three methods, the flux-corrected phase-field method is the most accurate in capturing the evolution of the shapes and performs the best in reducing shrinkage, coarsening and false merging effects. In addition, results also show that the flux-corrected phase-field method is not sensitive to the choice of the interfacial profile, due to the removal of the competition in the profile-corrected phase-field method, and hence is more robust.

Acknowledgments

This work is partially supported by the Hong Kong Research Grants Council under Competitive Earmarked Research Grant No. 621213.

References

[1] Wheeler, A., Murray, B., Schaefer, R.: Computation of dendrites using a phase field model. Physica D: Nonlinear Phenomena 66(1), 243-262 (1993).
[2] Cahn, J.W., Hilliard, J.E.: Free energy of a nonuniform system. I. Interfacial free energy. The Journal of chemical physics 28(2), 258-267 (1958).
[3] Warren, J.A., Boettinger, W.J.: Prediction of dendritic growth and microsegregation patterns in a binary alloy using the phase-field method. Acta Metallurgica et Materialia 43(2), 689-703 (1995).
[4] Beckermann, C., Diepers, H.-J., Steinbach, I., Karma, A., Tong, X.: Modeling melt convection in phase-field simulations of solidification. Journal of Computational Physics 154(2), 468-496 (1999).
[5] Karma, A., Rappel, W.-J.: Phase-field method for computationally efficient modeling of solidification with arbitrary interface kinetics. Physical Review E 53(4), R3017 (1996).
[6] Boettinger, W., Warren, J., Beckermann, C., Karma, A.: Phase-field simulation of solidification 1. Annual review of materials research 32(1), 163-194 (2002).
[7] Koyama, T.: Phase-field modeling of microstructure evolutions in magnetic materials. Science and Technology of Advanced Materials 9(1) (2008).

https://doi.org/10.4208/cicp.OA-2016-0150 Published online by Cambridge University Press

[8] Chen, L.-Q.: Phase-field models for microstructure evolution. Annual review of materials research 32(1), 113-140 (2002).
[9] Jacqmin, D.: Calculation of two-phase Navier-Stokes flows using phase-field modeling. Journal of Computational Physics 155(1), 96-127 (1999).
[10] Steinbach, I., Pezzolla, F., Nestler, B., Seeelberg, M., Prieler, R., Schmitz, G., Rezende, J.: A phase field concept for multiphase systems. Physica D: Nonlinear Phenomena 94(3), 135-147 (1996).
[11] Liu, C., Shen, J.: A phase field model for the mixture of two incompressible fluids and its approximation by a Fourier-spectral method. Physica D: Nonlinear Phenomena 179(3), 211-228 (2003).
[12] Bhate, D.N., Kumar, A., Bower, A.F.: Diffuse interface model for electromigration and stress voiding. Journal of Applied Physics 87(4), 1712-1721 (2000).
[13] Torabi, S., Lowengrub, J., Voigt, A., Wise, S.: A new phase-field model for strongly anisotropic systems. In: Proceedings of the Royal Society of London A: Mathematical, Physical and Engineering Sciences 2009, pp. 1337-1359.
[14] Jiang, W., Bao, W., Thompson, C.V., Srolovitz, D.J.: Phase field approach for simulating solid-state dewetting problems. Acta materialia 60(15), 5578-5592 (2012).
[15] Yeon, D.-H., Cha, P.-R., Grant, M.: Phase field model of stress-induced surface instabilities: Surface diffusion. Acta materialia 54(6), 1623-1630 (2006).
[16] Mahadevan, M., Bradley, R.M.: Phase field model of surface electromigration in single crystal metal thin films. Physica D: Nonlinear Phenomena 126(3), 201-213 (1999).
[17] Wise, S., Kim, J., Lowengrub, J.: Solving the regularized, strongly anisotropic Cahn-Hilliard equation by an adaptive nonlinear multigrid method. Journal of Computational Physics 226(1), 414-446 (2007).
[18] Rätz, A., Ribalta, A., Voigt, A.: Surface evolution of elastically stressed films under deposition by a diffuse interface model. Journal of Computational Physics 214(1), 187-208 (2006).
[19] Cahn, J.W., Elliott, C.M., Novick-Cohen, A.: The Cahn-Hilliard equation with a concentration dependent mobility: motion by minus the Laplacian of the mean curvature. European journal of applied mathematics 7(03), 287-301 (1996).
[20] Cahn, J.W., Taylor, J.: Surface motion by surface diffusion. Acta Metallurgica et Materialia 42(4), 1045-1063 (1994).
[21] Lee, A.A., Muünch, A., Süli, E.: Sharp-Interface Limits of the Cahn-Hilliard Equation with Degenerate Mobility. SIAM Journal on Applied Mathematics 76(2), 433-456 (2016).
[22] Lee, A.A., Münch, A., Süli, E.: Degenerate mobilities in phase field models are insufficient to capture surface diffusion. Applied Physics Letters 107(8), 081603 (2015).
[23] Dai, S., Du, Q.: Coarsening Mechanism for Systems Governed by the Cahn-Hilliard Equation with Degenerate Diffusion Mobility. Multiscale Modeling & Simulation 12(4), 1870-1889 (2014).
[24] Yue, P., Zhou, C., Feng, J.J.: Spontaneous shrinkage of drops and mass conservation in phase-field simulations. Journal of Computational Physics 223(1), 1-9 (2007).
[25] Li, Y., Choi, J.-I., Kim, J.: A phase-field fluid modeling and computation with interfacial profile correction term. Communications in Nonlinear Science and Numerical Simulation 30(1), 84-100 (2016).
[26] Macklin, P., Lowengrub, J.: Evolving interfaces via gradients of geometry-dependent interior Poisson problems: application to tumor growth. Journal of Computational Physics 203(1), 191-220 (2005). doi:10.1016/j.jcp.2004.08.010.
[27] Macklin, P., Lowengrub, J.: An improved geometry-aware curvature discretization for level

https://doi.org/10.4208/cicp.OA-2016-0150 Published online by Cambridge University Press

set methods: application to tumor growth. Journal of Computational Physics 215(2), 392-401 (2006).
[28] Salac, D., Lu, W.: A Local Semi-Implicit Level-Set Method for Interface Motion. Journal of Scientific Computing 35(2-3), 330-349 (2008). doi:10.1007/s10915-008-9188-6.
[29] Ervik, Å., Lervåg, K.Y., Munkejord, S.T.: A robust method for calculating interface curvature and normal vectors using an extracted local level set. Journal of Computational Physics 257, 259-277 (2014). doi:10.1016/j.jcp.2013.09.053.
[30] Lervåg, K.Y.: Calculation of interface curvature with the level-set method. in: Sixth National Conference on Computational Mechanics MekIT11, Trondheim, Norway (2011).
[31] Gugenberger, C., Spatschek, R., Kassner, K.: Comparison of phase-field models for surface diffusion. Physical Review E 78(1), 016703 (2008).
[32] Yue, P., Feng, J.J., Liu, C., Shen, J.: A diffuse-interface method for simulating two-phase flows of complex fluids. Journal of Fluid Mechanics 515, 293-317 (2004).
[33] FFTW Homepage Website. http://www.fftw.org.
[34] Sudoh, K., Iwasaki, H., Kuribayashi, H., Hiruta, R., Shimizu, R.: Numerical Study on Shape Transformation of Silicon Trenches by High-Temperature Hydrogen Annealing. Japanese Journal of Applied Physics 43(9A), 5937-5941 (2004). doi:10.1143/jjap.43.5937.
[35] Zhang, Y., Ye, W.: A High-Order Level-Set Method with Enhanced Stability for Curvature Driven Flows and Surface Diffusion Motion. Journal of Scientific Computing, 1-30 (2016).
[36] Kolahdouz, E.M., Salac, D.: A Semi-implicit Gradient Augmented Level Set Method. SIAM Journal on Scientific Computing 35(1), A231-A254 (2013). doi:10.1137/120871237.

https://doi.org/10.4208/cicp.OA-2016-0150 Published online by Cambridge University Press